N73-21812

NASA TECHNICAL MEMORANDUM

NASA TM X-64738

CASE FILE COPY

STRUCTURAL LOAD REDUCTION OF THE SPACE SHUTTLE BOOSTER/ORBITER CONFIGURATION USING A LOAD RELIEF GUIDANCE TECHNIQUE

By A. W. Deaton and P. B. Kelley
Aero-Astrodynamics Laboratory

April 5, 1973

NASA

George C. Marshall Space Flight Center
Marshall Space Flight Center, Alabama

MSFC - Form 3190 (Rev June 1971)

TECHNICAL REPORT STANDARD TITLE PAGE

1. REPORT NO. NASA TM X-64738	2. GOVERNMENT ACCESSION NO.	3. RECIPIENT'S CATALOG NO.
4. TITLE AND SUBTITLE Structural Load Reduction of the Space Shuttle Booster/Orbiter Configuration Using a Load Relief Guidance Technique		5. REPORT DATE April 5, 1973 6. PERFORMING ORGANIZATION CODE
7. AUTHOR(S) A. W. Deaton and P. B. Kelley*		8. PERFORMING ORGANIZATION REPORT #
9. PERFORMING ORGANIZATION NAME AND ADDRESS George C. Marshall Space Flight Center Marshall Space Flight Center, Alabama 35812		10. WORK UNIT NO. 11. CONTRACT OR GRANT NO.
12. SPONSORING AGENCY NAME AND ADDRESS National Aeronautics and Space Administration Washington, D. C. 20546		13. TYPE OF REPORT & PERIOD COVERED Technical Memorandum 14. SPONSORING AGENCY CODE

15. SUPPLEMENTARY NOTES

*Northrop Services, Inc.
Huntsville, Alabama

16. ABSTRACT

A space shuttle booster/orbiter atmospheric ascent guidance algorithm is developed that will reduce the aerodynamically induced structural loads as compared to an open loop guidance algorithm.

17. KEY WORDS	18. DISTRIBUTION STATEMENT Unclassified - Unlimited E. D. Geissler, Director Aero-Astrodynamics Laboratory

19. SECURITY CLASSIF. (of this report)	20. SECURITY CLASSIF. (of this page)	21. NO. OF PAGES	22. PRICE
Unclassified	Unclassified	35	NTIS

MSFC - Form 3292 (May 1969)

LIST OF ILLUSTRATIONS

TECHNICAL MEMORANDUM X-64738

STRUCTURAL LOAD REDUCTION OF THE SPACE SHUTTLE BOOSTER/ORBITER CONFIGURATION USING A LOAD RELIEF GUIDANCE TECHNIQUE

SUMMARY

This report discusses a trajectory shaping technique that can be used by the space shuttle booster/orbiter configuration to reduce the aerodynamically induced structural loads during booster ascent and develops this concept into a load relief guidance scheme. The guidance feasibility analysis of this guidance scheme has shown that the structural loads can be reduced by as much as a factor of 2 when compared to the open loop (time dependent) guidance scheme based upon steady state moment balance trajectory simulations. The load relief guidance algorithm developed in this report has been applied only to the pitch plane steering with yaw steering set equal to zero.

I. INTRODUCTION

The purpose of this report is to describe a space shuttle booster and orbiter atmospheric ascent guidance system that will reduce the aerodynamically induced structural loads caused by thrust perturbations and flight winds as compared to the traditional open loop (time dependent) guidance technique. In order to reduce loads induced by inflight perturbations, the scheme has to be an adaptive guidance algorithm. This is accomplished by using measured inertial pitch plane velocity components as parameters in the closed-loop generation of the pitch steering commands. This particular load relief guidance technique considered (1) load reduction, (2) simplicity of on-board implementation, and (3) orbiter computer storage requirements as the major objectives. The rationale behind the selection of the functional form for the load relief guidance equations will be developed, and the results of a brief feasibility analysis will be presented which demonstrate the capability of the guidance system to handle vehicular and atmospheric perturbations during the booster/orbiter ascent portion of flight. All booster/orbiter trajectories in the feasibility analysis were simulated assuming steady-state moment balance and perfect booster/orbiter control.

This guidance algorithm was developed only for the pitch plane, and yaw steering was set equal to zero during the atmospheric ascent portion of flight. Active yaw steering was initiated shortly after booster cutoff when vacuum assumptions were valid for optimum steering (maximum orbital insertion weight).

The following subjects will be discussed in this report:

1. Trajectory Shaping Technique
2. Open Loop Guidance Scheme
3. Wind Biasing
4. Development of Closed Loop Atmospheric Ascent Guidance Scheme
5. Load Relief Guidance Feasibility Analysis

This guidance feasibility analysis indicates that a significant reduction in the aerodynamically induced structural loads can be achieved by using a closed-loop guidance system during space shuttle atmospheric ascent as compared to an open-loop guidance system. The structural loads indicator (dynamic pressure times Δ angle of attack) has been reduced by a factor of 4 in some special cases and a factor of 2 in other special cases. An MSFC pressure-fed booster/orbiter configuration was used to make this feasibility analysis; but the load relieving feature of the guidance function should be applicable to the latest ATP (Authority To Proceed) space shuttle configuration which uses recoverable solid rocket motors as the booster stage.

II. DISCUSSION OF TRAJECTORY SHAPING AND WIND BIASING TECHNIQUES

Before going into very much detail about developing an atmospheric guidance algorithm that will give structural load relief, it is almost mandatory that a short discussion of trajectory shaping be given since the two subjects are so intricately interwoven in concept and objective. In the past, the trajectory shaping technique used for generating launch vehicle trajectories was relatively simple since the launch vehicles were symmetrical in structural design (cylindrical) and the center of gravity was always near the structural centerline. Saturn trajectories were shaped by steering the vehicle in a vertical direction until launch tower clearance (10-12 seconds) and then introducing an angle of attack program to start the launch vehicle moving downrange. Angle of attack is defined as the angle between the vehicle centerline and the relative velocity vector. The angle-of-attack program consisted of linearly building the angle of attack up to some constant value and holding it constant for a specified time. Next, this constant angle of attack was linearly decreased to zero approximately 40 seconds prior to maximum dynamic pressure. The angle of attack was held at zero (gravity turn) until inboard engine cutoff. At this point, the attitude (steering angle) was held constant to allow first stage cutoff and separation to occur from a rotational-free state. Shortly after second stage ignition, the vehicle steering angles were determined by a guidance program (IGM [1,2,3]) that would allow orbital insertion to occur at near minimum fuel expenditure. The trajectory shaping technique consisted of determining the constant angle of attack that would yield the maximum payload delivered to earth parking orbit. The resulting first stage steering profile was curve fit with respect to time and implemented as an open-loop steering program [$\chi_p = f(\text{time})$]. This shaping technique allowed the launch vehicle to tilt over and then follow a zero angle-of-attack trajectory profile through the high dynamic pressure region of flight, thus minimizing the control problems during this critical region of flight. Since the Saturn launch vehicles were cylindrical, zero angle of attack also meant zero normal aerodynamic forces. The launch (flight) azimuth was selected so that yaw (lateral) steering in the first stage could be set equal to zero.

The next concept that must be understood before going into the load relief discussion is the technique of wind biasing the trajectory for the predicted launch wind. Wind effects appear in the equations of motion through the space-fixed relative velocity vector equation ($\overline{VR} = \dot{\overline{R}} - \overline{\Omega} \times \overline{R} - \overline{WIND}$). Wind vectors are given as a function of altitude. The wind azimuth and wind speed as a function of altitude for a Cape Kennedy launch site "December, January, February, and March seasonal wind" based upon several years of statistics (References 4 and 5) are given in Figure 1. It is easy to see that if the wind vector is used in the relative velocity equation, a trajectory can be shaped that will result in a zero angle of attack profile provided that the wind vector history selected does, indeed, exist on that particular launch day. The trajectory will be tuned to that particular wind vector history. The pitfalls to wind biasing are serious. If the open-loop steering program has been determined from a particular predicted wind history (azimuth and wind speed profile), and no wind or some other wind history exists for that launch day, then an angle of attack other than zero will be present through the high dynamic pressure region of flight. This will cause high aerodynamically induced normal forces on the launch vehicle and require the control system to gimbal the engines to balance the thrust and aerodynamic moments. Additional vehicle related perturbations coupled with the wind problem can cause loss of control authority and mission failure.

The message is quite clear that great care and conservatism should be exercised if wind biasing techniques are used to reduce aerodynamically induced structural loads.

With the first stage trajectory shaping and wind biasing concepts in mind, the discussion will shift to applying these concepts to the non-symmetrical lifting body configuration of the space shuttle. The basic Saturn launch vehicle trajectory shaping techniques can also be

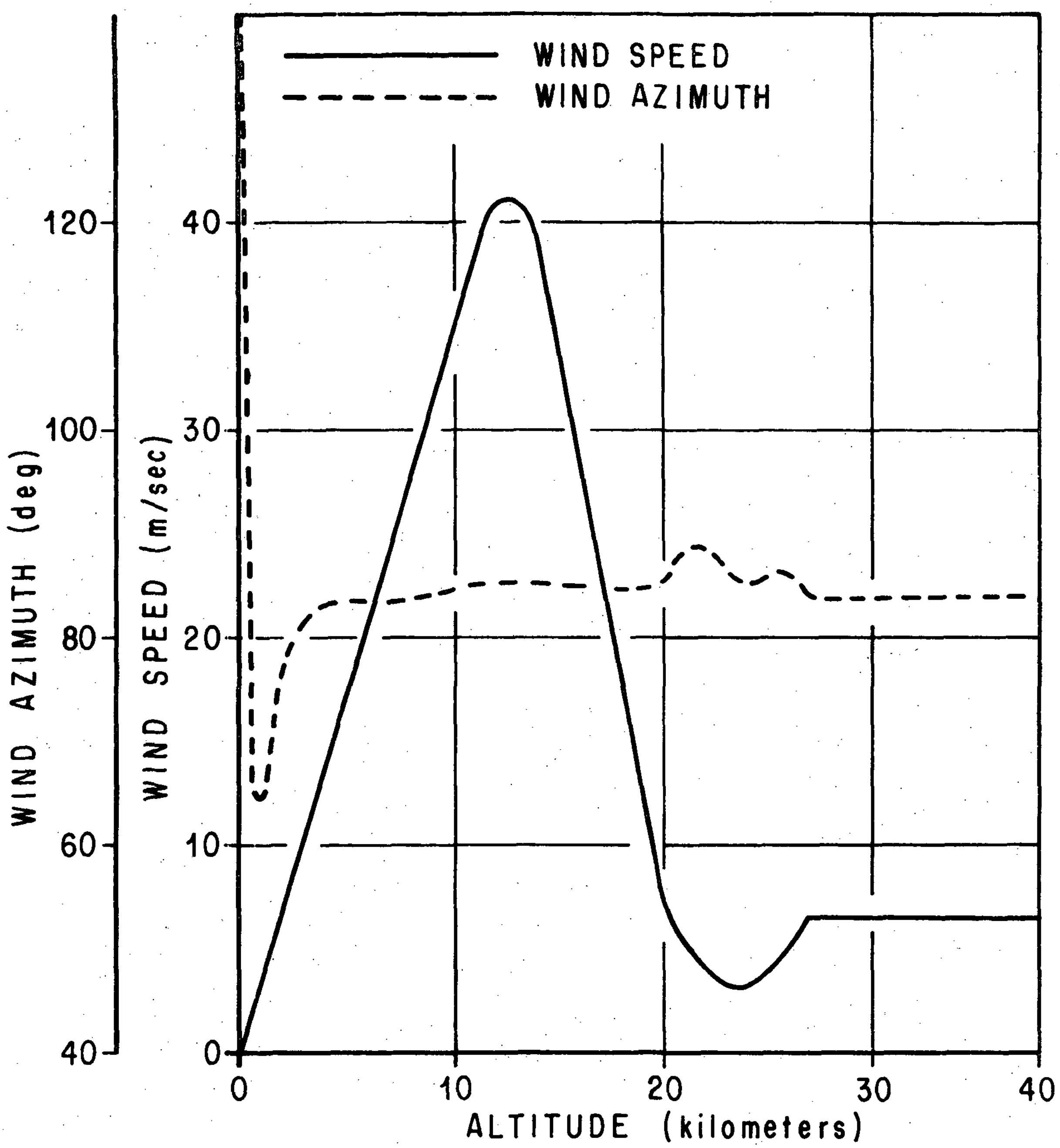

FIG. 1. MEAN VECTOR WIND FOR DEC., JAN., FEB., MAR. CAPE KENNEDY, FLORIDA

applied to the space shuttle provided certain aerodynamic characteristics and configuration differences are properly treated in the trajectory design. The feasibility analysis presented herein used the MSFC pressure-fed booster configuration, since, once the analysis was started, it was virtually impossible to keep up with day to day changes in the configuration of the space shuttle. Since all proposed space shuttle configurations represent non-symmetrical bodies, zero angle of attack does not result in zero aerodynamic normal forces. The zero lift angle-of-attack profiles for these bodies are given as a function of Mach number (velocity divided by the speed of sound). Also, zero lift angle of attack does not represent zero aerodynamic moment.

The location of the center of gravity (CG) away from the centerline of the booster will require the engines to gimbal to track the center of gravity during atmospheric ascent (Figure 2-A). Also, non-symmetrical engine locations will require the orbiter engines to gimbal during ascent to track the CG (Figure 2-B). This means that the thrust vector will not be directed along the vehicle centerline and will give a crabbed appearance during the vertical rise at liftoff (the centerline of the configuration will not be 90 degrees with respect to the horizontal).

The trajectory shaping techniques used to establish the space shuttle vehicle attitude through the atmospheric ascent will require gimbaling of the control engines so that steady-state moment balance conditions will exist at any time during flight. This will permit the resultant thrust vector to track the CG when the aerodynamic forces are near zero at liftoff and balance the aerodynamic and thrust moments during the tilt-over (angle-of-attack program) phase of flight. After the tilt-over phase of flight, the angle-of-attack program can be blended into the zero lift angle-of-attack state (α_{ZL} is a function of Mach number) prior to experiencing maximum dynamic pressure in the trajectory. The vehicle centerline will follow this zero-lift angle-of-attack state until shortly after booster cutoff while maintaining steady state moment balance. The remainder of the vehicle attitude history will be established using a calculus of variations computer subroutine to maximize the orbital insertion weight. The final trajectory shape is established by numerically determining the tilt-over angle-of-attack program that will yield maximum cutoff weight at orbital insertion (50 x 100 n. mi.). An illustration of this technique is shown on Figure 3 in which the steering attitude (angle between the space-fixed horizontal at liftoff and the vehicle centerline) and angle-of-attack program are plotted against time for the first 120 seconds of flight. Failure to use steady state moment balance conditions can cause the space shuttle to encounter severe dynamics and control problems as well as large payload losses when the trajectory simulation makes use of a full 6 degrees of freedom and active control system.

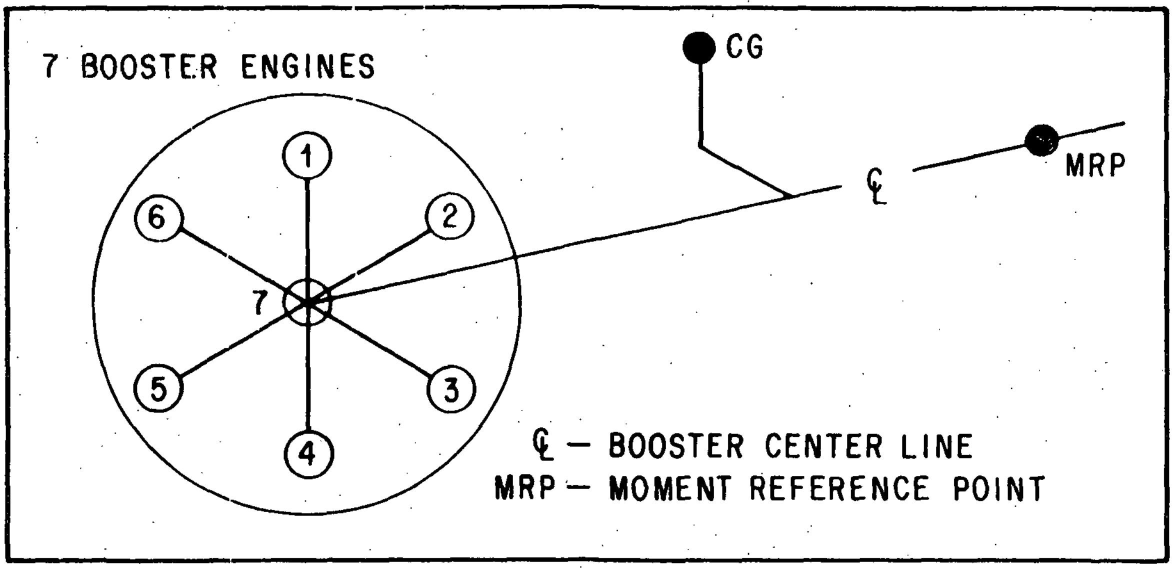

FIG. 2a. MSFC PRESSURE-FED BOOSTER/ORBITER CONFIGURATION

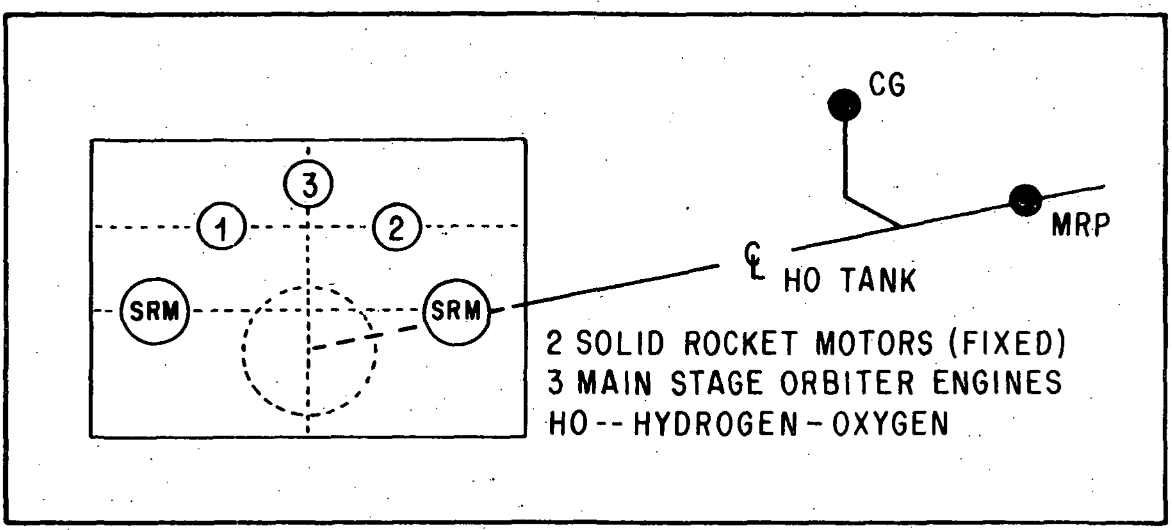

FIG. 2b. SRM PARALLEL BURN BOOSTER/ORBITER ATP CONFIGURATION

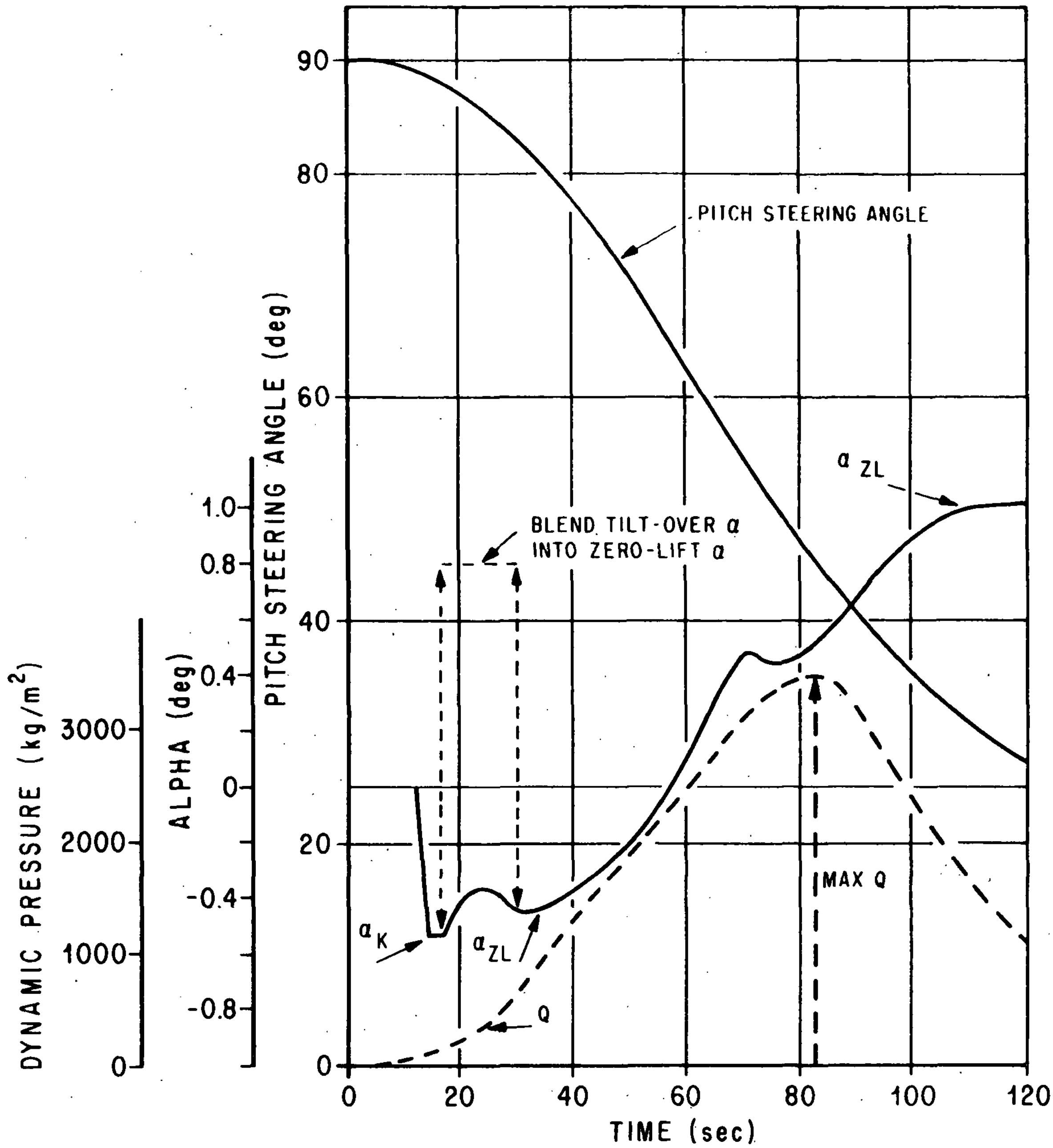

FIG. 3. TRAJECTORY SHAPING FOR NOMINAL

The wind biasing techniques described earlier can be used for the space shuttle. Since the pitch steering problem seems to be the most critical area of concern, emphasis was placed on this problem solution and the yaw steering problems were neglected for the time being.

III. SELECTION OF VARIABLES AND FUNCTIONAL FORM

Now that trajectory shaping has been treated, the discussion will shift to the selection of the functional form of a load relief guidance scheme and the variables to be used in the guidance equations. As stated earlier, the selection of the guidance scheme will be heavily influenced by simplicity of the scheme and the capability of the scheme to respond favorably to vehicular or atmospheric perturbations. Also, the relationship between the guidance and control system must be understood before selecting the variables that should go into an atmospheric ascent guidance scheme so that guidance and control interactions can be avoided whenever possible. It will be the function of the space shuttle control system to keep the vehicle's centerline near the commanded attitude (pitch and yaw steering commands) throughout the flight. The space shuttle control system must react to short term perturbations in vehicular (thrust, Isp, thrust unbalance, etc.) and atmospheric (wind, wind gust and shears, density variations, etc.) anomalies that can cause a torque on the vehicle and a drift away from the commanded steering program. The control equation of a space vehicle usually takes the following form:

$$\beta = A_o(\Delta X) + A_1(\Delta\dot{X}) + B_o(\alpha) + g_2(\ddot{\gamma}),$$

where β is defined to be the engine deflection angle,

A_o the attitude control gain,

A_1 the attitude rate control gain,

B_o the angle of attack control gain, and

g_2 the accelerometer control gain.

Load relief can be obtained with this formulation of the control equation through proper gain scheduling of the B_o of g_2 gains. In general, only B_o (angle of attack control) or g_2 (lateral acceleration control) will be used and not both at once. The g_2 gain uses the output from a body mounted accelerometer to detect structural loads and allows the attitude of the vehicle to drift in the proper direction to reduce the lateral acceleration. The B_o gain uses the output from an angle of attack meter (angle of attack may be derived from a Q-ball instrument) and reduces the structural load by allowing the vehicle to drift into the wind. A detailed discussion of the control system and the control equations is outside the scope of this report and only mentioned to make the reader aware that load relief for the short term perturbation is available through the control system. But, once the trajectory history (time, displacement and velocity vectors) has been altered by some perturbation, the steering commands should be modified to allow the remainder of the trajectory to be flown in an acceptable compromise between structural loads and payload to be delivered to orbit.

The information available from the space shuttle navigation system that could be used in developing a load relief guidance scheme is space-fixed earth-centered displacement and velocity vectors, acceleration (F/M), and time. Measured acceleration is subject to high levels of noise and must be smoothed by a filter before it can be used in a guidance system. A guidance scheme that uses measured acceleration always responds rapidly to any deviation to the nominal acceleration and runs the risk of coupling with the control system or amplifying a propellant slosh problem (if liquid propellants are used). Time from liftoff could be used in the guidance formulation, but time does not give any trajectory history information that could be used in the guidance equation development to reduce structural loads.

Displacement is a candidate variable for a load relief guidance function since it is a slow responding parameter. A perturbation is first sensed through the integrating accelerometer output in terms of an off-nominal velocity increment. After combining the inertial velocity obtained from the integrating accelerometers with the velocity due to the gravitational potential, the velocity is integrated to give displacement. A trajectory perturbation is first detected through an acceleration deviation, then through velocity, and finally, through displacement. Since the displacement vector is so slow in detecting a trajectory perturbation by itself, it will be eliminated as a candidate variable in this particular analysis. Further discussion as to how this displacement vector can be used in formulating the guidance equations will be given later in this report.

The most likely candidate variables for consideration in the formulation of the guidance equations are the velocity vector components in the pitch plane since a perturbation is sensed in velocity only after sufficient time has elapsed to let the integrated effect be accumulated in the navigational state. And since there is a natural time lag built into the velocity vector computation, there is very little danger in a guidance and control coupling problem causing any difficulty in atmospheric flights. Since velocity shows up in the relative velocity vector equation

($\overline{VR} = \dot{\overline{R}} - \overline{\omega} \times \overline{R} - \overline{WIND}$, where $\overline{R} = x\hat{i} + y\hat{j} + z\hat{k}$ and
$\dot{\overline{R}} = \dot{x}\hat{i} + \dot{y}\hat{j} + \dot{z}\hat{k}$)

and the relative velocity vector is used in the trajectory shaping technique, it is logical to use the inplane pitch components of velocity to formulate the guidance equations (yaw steering is set equal to zero). It should be straightforward to relate a change in velocity to a change in the pitch steering command, since velocity is used in the trajectory shaping technique.

The discussion will now shift to the technique used to formulate a set of guidance equations that uses velocity components in the pitch plane as the basis for determining the pitch steering commands that will offer structural load relief. There are many ways to attack this problem, but the approach chosen in this report is to use a technique that very closely coincides with the trajectory shaping philosophy of the space shuttle atmospheric ascent flight. The vehicle perturbations (3-sigma value) that most seriously affects the aerodynamically induced structural loads is the thrust uncertainty since a low or high thrust level will change the acceleration history of that particular stage, and, consequently, the velocity history which determines angle of attack. Of course, the external disturbances causing the largest aerodynamically induced loads are wind, wind gust, and wind shears.

If a space shuttle atmospheric ascent trajectory is shaped according to the techniques outlined earlier in the discussion for a prior knowledge of a low or high thrust (±4% F) during the booster flight, the pitch steering profiles and corresponding angle-of-attack profiles will take the forms shown in Figure 4. The ±4% thrust level deviations from the nominal value are not necessarily 3-sigma uncertainty values, but are representative of what might be expected from the propulsion system. The angle-of-attack tilt-over program begins at 10 seconds after liftoff for the +4% F case, 12 seconds for the nominal case, and 14 seconds for the -4% F case, which is typical, if the tower clearance constraint is to be satisfied. The angle-of-attack tilt-over program is blended into the zero lift angle-of-attack profile at 30 seconds into the flight. The pitch steering profiles that correspond to these optimum angle-of-attack tilt-over programs are also shown on Figure 4. The pitch profile for the nominal thrust level is centered between the ±4% F cases.

Since the velocity components in the pitch plane have been selected as the most deisrable variables to be used in formulating a closed-loop pitch steering system, the inertial pitch plane velocity components ($\dot{X}$ is the space-fixed vertical component and $\dot{Z}$ is the space-fixed downrange component) are given for the ±4% F cases by Figure 5. The inertial velocity components were selected rather than the total space-fixed velocity components ($\dot{\bar{X}}_S = \dot{\bar{X}} + \dot{\bar{X}}_g$) because a perturbation will show up in the form of a deviation from the nominal sooner in that particular frame of reference. Inertial velocity is the output from the integrating acceleration which measures the effects of the physical forces acting on the vehicle (gravity contribution to the total space-fixed velocity is computed). It should be noted that for the first 50 seconds of flight

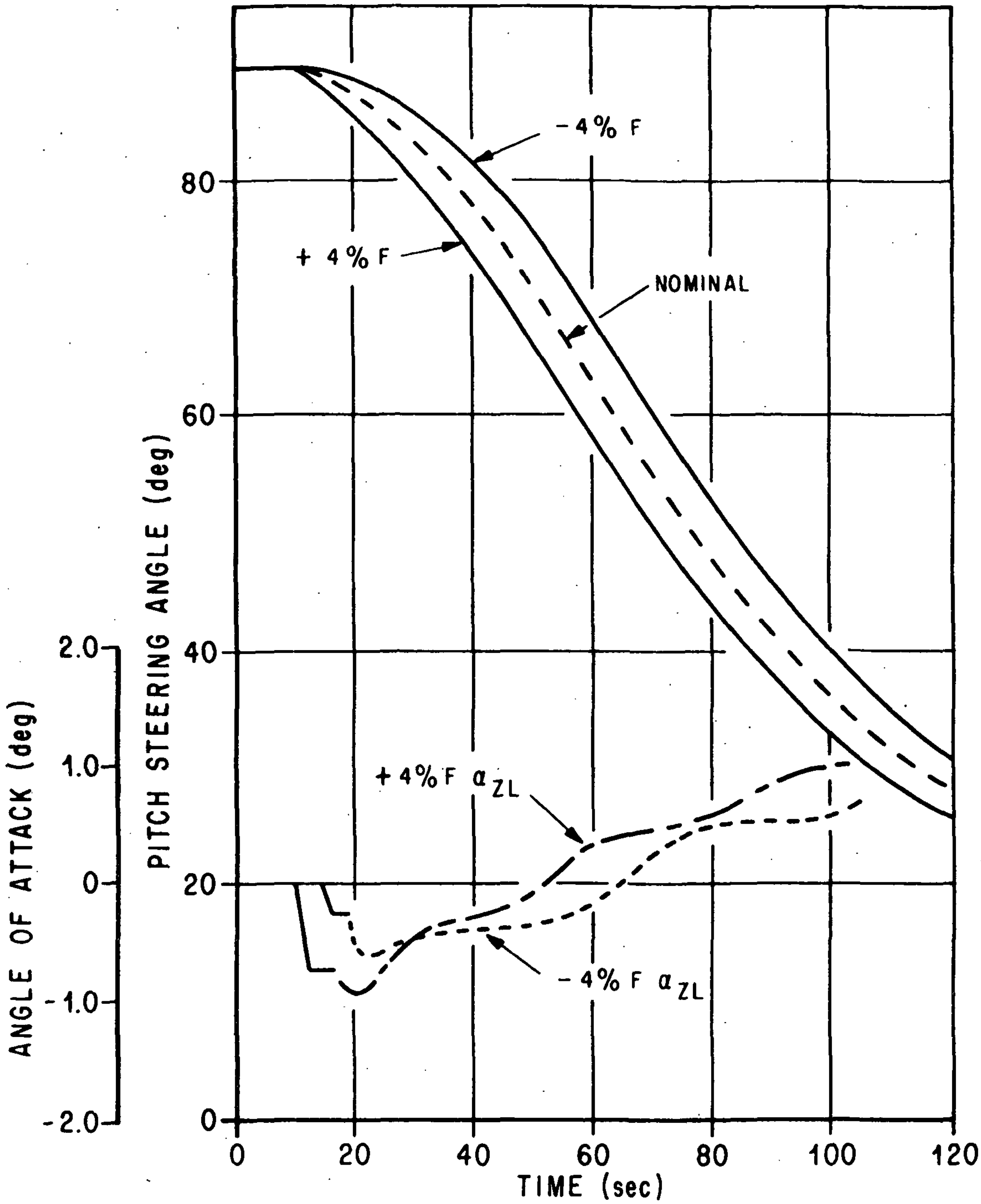

FIG. 4. ± 4% F BOUNDARY CURVES

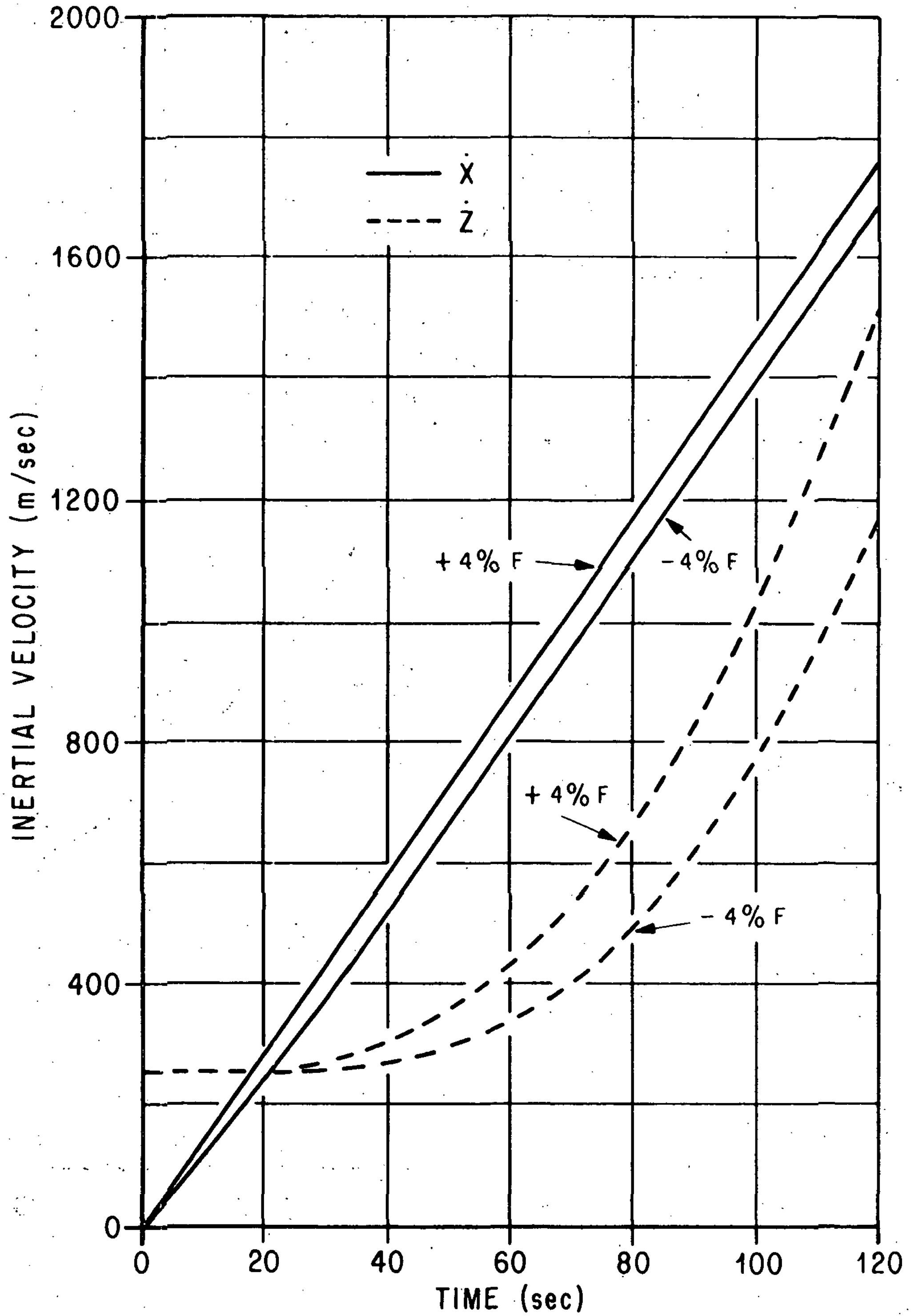

FIG. 5. ± 4% F PITCH PLANE INERTIAL VELOCITY

most of the velocity change is in the vertical direction and after that time there is a fast rate of change in the horizontal (downrange) velocity ($\dot{Z}$).

The problem of how to relate these velocity histories to the pitch steering commands and still conserve the trajectory shaping philosophy built into the design of these trajectories will now be addressed. The pitch steering command (χ_p) can be related to these parameters of inplane pitch velocity components (selected for response characteristics) by the following functional representation.

$$\chi_P = f(\dot{X}, \dot{Z}, t), \quad \text{or}$$

$$\chi_P = f(\Delta),$$

$$\text{where} \quad \Delta = \dot{Z} + N(t)\dot{X} + C(t)t,$$

and where $N(t)$ is a time varying coefficient that is chosen such that the steering commands are correlated with the velocity history and $C(t)$ is an open loop time coefficient (may or may not be constant).

The "C(t)t" term in the Δ equation is an open loop parameter that should be used in the formulation since the early portion of flight is basically open loop (the steering program is totally a function of time and not modified by the navigational state). After tower clearance and kick-over (tilt-over) to start the vehicle moving downrange, the navigational state should then become more important in determining the steering attitude angles and the "Ct" term should be reduced in magnitude. The coefficient "C(t)" should be a time varying coefficient (possibly linearly decreasing with time) that diminishes in importance as time increases. The coefficients "C(t)" and "N(t)" have the units required to agree with the Δ variable (meters per second).

The numerical technique used to determine $f(\Delta)$ and $N(t)$ is basically a data processing procedure that requires a certain amount of engineering judgement and knowledge of the objectives of the resulting guidance algorithm. The procedure for determining Δ and $N(t)$ is graphically illustrated by Figure 6 in which the pitch steering profiles for the ±4% booster thrust deviations from the nominal are plotted against time from liftoff. By assigning an arbitrary value to the new variable (Δ) at the beginning of the shuttle tilt-over (point A), it is possible to compute $N(t_A)$ since

$$\Delta_A = \dot{Z}_A + N(t_A)\dot{X}_A + C(t_A)t_A, \text{ and } \dot{Z}_A, \dot{X}_A \text{ and } t_A$$

are known from trajectory data and $C(t)$ is a pre-assigned function of t. Also, since Δ_A must equal Δ_B (χ_p at point A equals χ_p at point B), then

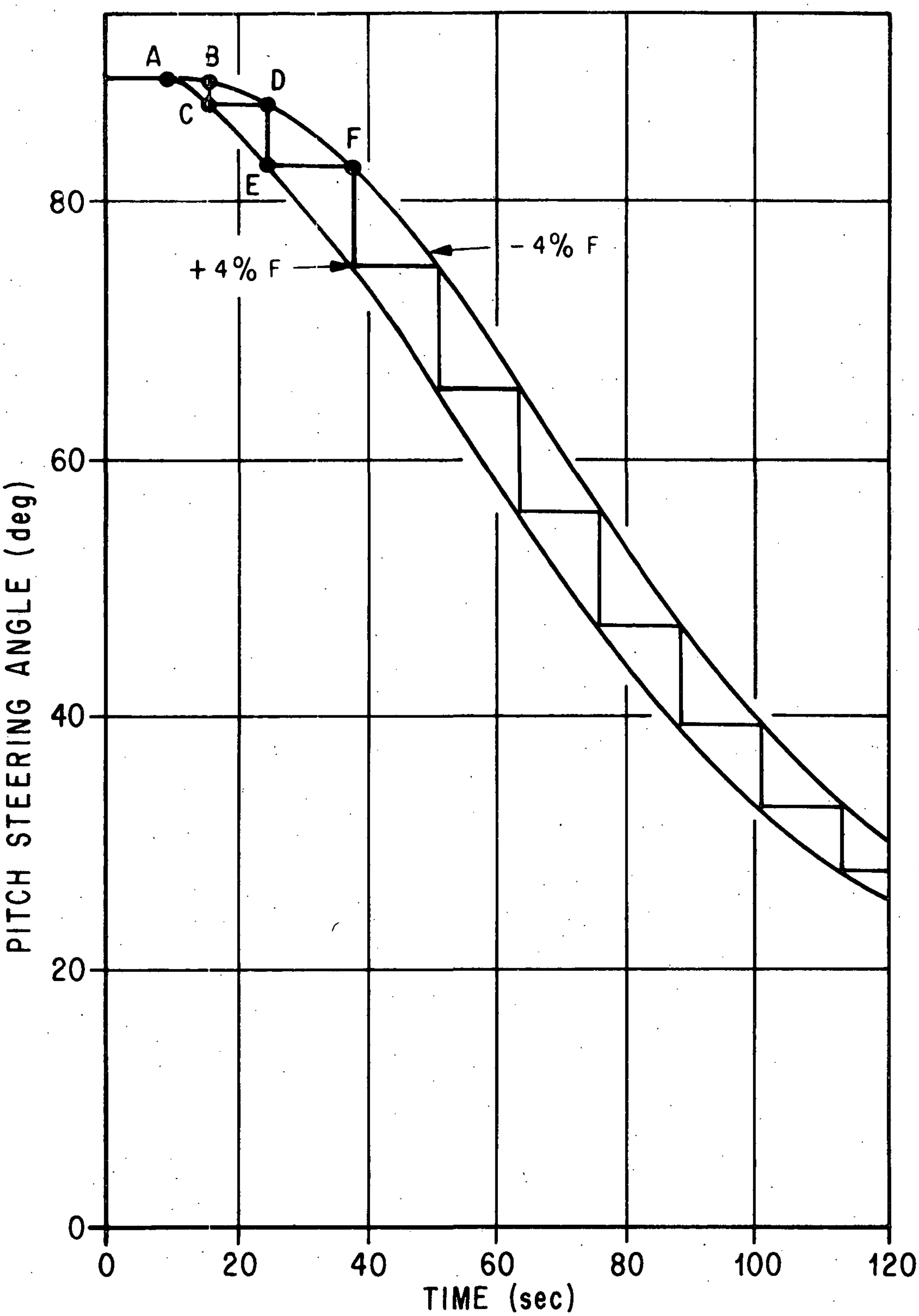

FIG. 6. Δ AND N(t) COMPUTATION

$N(t_B)$ can be computed from $\Delta_A = \Delta_B$ or

$$\dot{Z}_A + N(t_A)\dot{X}_A + C(t_A)t_A = \dot{Z}_B + N(t_B)\dot{X}_B + C(t_B)t_B$$

since $\dot{Z}_B$, $\dot{X}_B$, and t_B are also known. Δ at point C can be computed since t is the same for points B and C, thus $N(t_C)$ is now $[N(t_B)]$ and $\dot{X}_C$ and $\dot{Z}_C$ are known. In a similar fashion, the values for Δ and N(t) can be computed for the entire boost trajectory.

By assuming that Δ along the lower boundary trajectory varies linearly from point A (time = 10 seconds) to point C (time = 14 seconds), additional projection values of Δ (at 12 seconds as an example) can be used to insure that sufficient data will be available to adequately define the shape of N(t) from t = 10 seconds to booster cutoff. A judicious choice of a starting value of Δ at tilt-over of 1000 results in the extremely well behaved steering angle profile (Figure 7) plotted against the new variable, Δ, that relates the steering angle to the velocity while maintaining a load relief trajectory shaping philosophy. This particular starting value of Δ at tilt-over initiation makes it possible to avoid variable scaling problems for the flight computer (Δ varies from 800 at liftoff to 4000 at booster cutoff). The time varying coefficient, N(t), that corresponds to the Δ variable shown by Figure 7 is illustrated in Figure 8 with the open-loop coefficient "C(t)" equal to one (1.0).

The importance of "C(t)" in the variable Δ may not appear obvious to the reader. The open loop parameter "C(t)" can be thought of as an experience factor that can be used effectively to control the amount of response the designer wants the guidance system to possess during certain regions of flight. Suppose for instance that after a control analysis using full dynamics has been performed, the guidance response to a thrust perturbation at 30 to 35 seconds caused a temporary guidance and control interaction problem. It would be possible to get around this problem by assigning a higher value to "C(t)" during this region of flight and weakening the guidance response.

This particular load relief guidance technique allows the guidance and control system to be studied jointly in such a way that engineering judgement based on sound in-depth analysis can be incorporated into the final guidance and control system design.

Before going on to the steady state guidance analysis of this proposed guidance algorithm, a few comments about how this particular technique can be expanded to incorporate the inplane displacement components into the guidance formulation seems justified. To do this, the variable, Δ, might take on the following form:

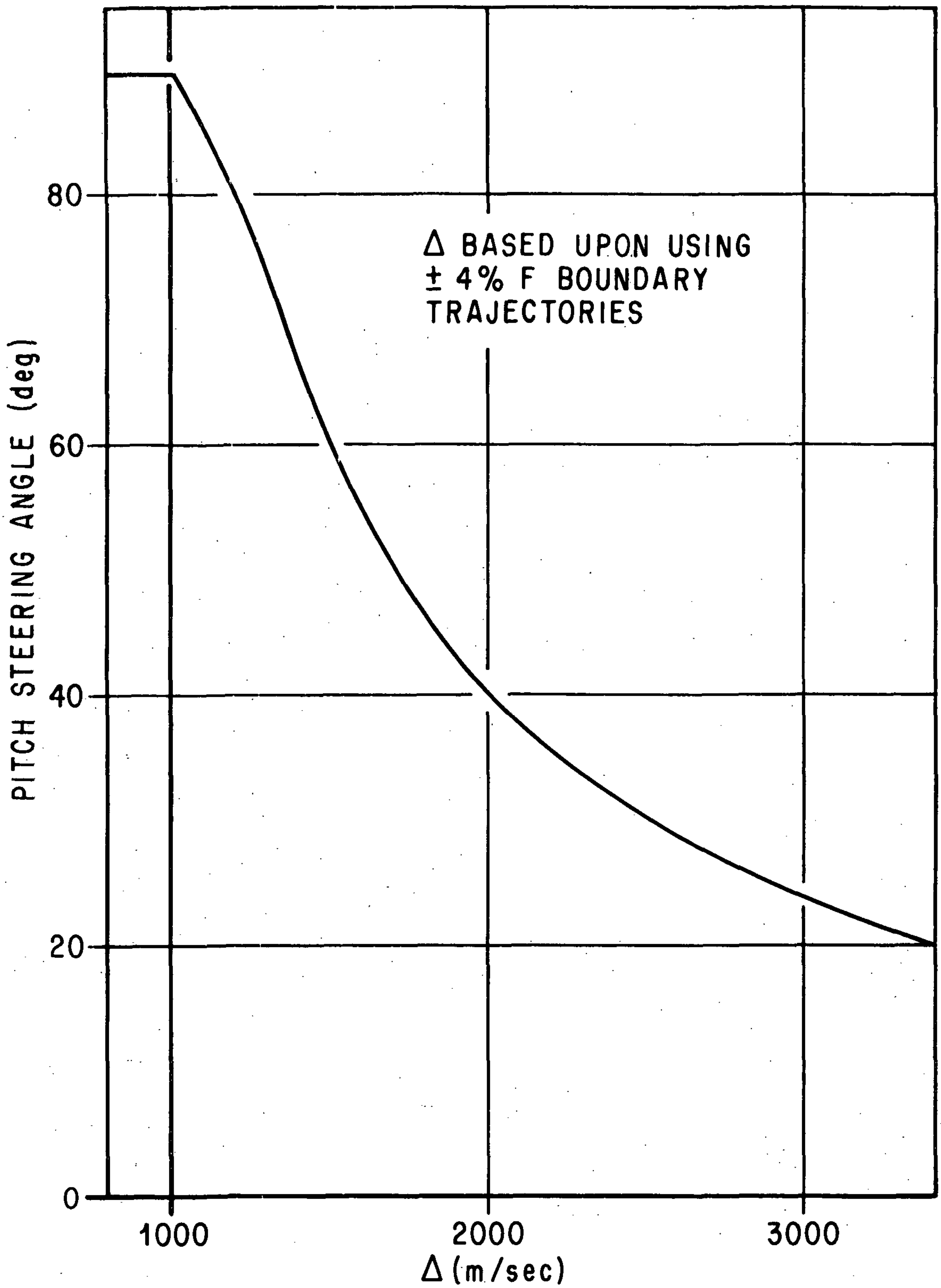

FIG. 7. PITCH STEERING ANGLE vs Δ

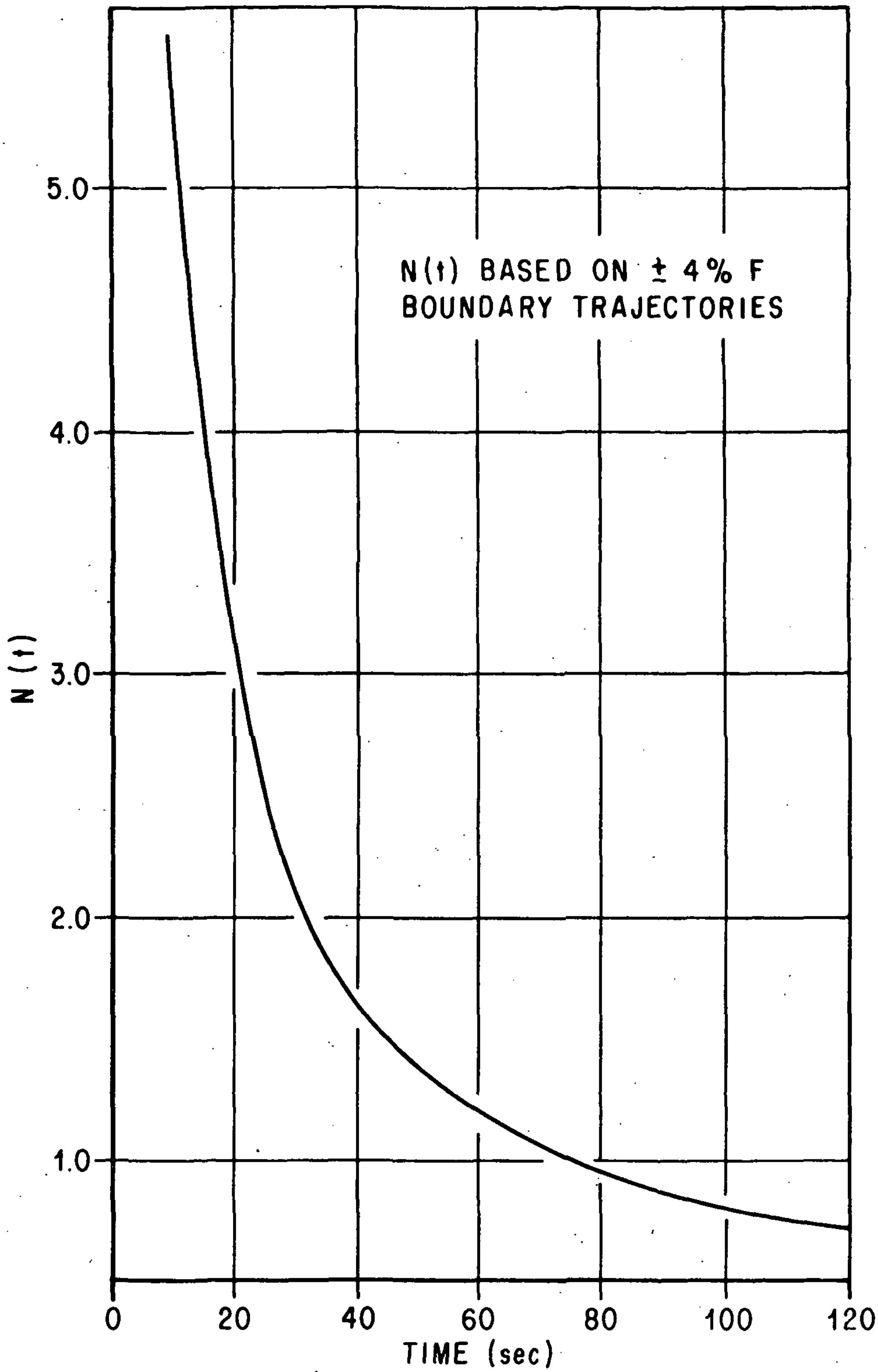

FIG. 8. N(t) COEFFICIENT

$$\Delta = \dot{Z} + N(t)\dot{X} + Z + M(t)X + C(t)t,$$

where Z is the downrange inertial displacement component,

X is the vertical inertial displacement component,

$M(t)$ is a time varying displacement coefficient,

and $\dot{Z}$, $\dot{X}$, $N(t)$, and $C(t)$ take on the same definition as before.

By using the same lower and upper boundary trajectories (±4% F) and a third trajectory (the nominal, see Figure 4), a similar numerical projection technique can be established that will relate the pitch steering angle to the velocity and displacement navigational state. The load relief trajectory shaping technique used to generate these trajectories will dictate the guidance algorithm response to trajectory perturbations.

There are many approaches that can be taken to solving the space shuttle atmospheric guidance problem, but this particular approach was taken because of its simplicity, ease of implementation, and capability of incorporating engineering analysis results into the function design. The idea for developing this guidance technique comes from Reference 6 in which a similar technique was applied to the first stage Saturn launch vehicle engine-out problem.

IV. STEADY-STATE MOMENT-BALANCE ATMOSPHERIC GUIDANCE ANALYSIS

This section of the report will describe the trajectory simulations that were used to establish feasibility of this structural load relief guidance concept and outline the plan of attack in applying this technique to the latest space shuttle solid rocket motor booster/orbiter configuration. The load relief guidance feasibility analysis will consist of comparing the maximum loads indicator (MAX $Q\Delta\alpha$) from this velocity closed-loop guidance system to the open-loop (time dependent) guidance system for both wind biased and non-wind biased trajectories.

The space shuttle simulation computer program that was used for this analysis is illustrated in block diagram form by Figure 9. This analysis is based upon using a perfect control assumption (actual vehicle attitude is equal to the commanded vehicle attitude) and steady-state moment balance in which the engine gimbal angles are computed that will balance the aerodynamic and thrust moments. In a trajectory simulation in which full dynamics are used, the control system would use the commanded steering angles ($\overline{\chi_p}$, $\overline{\chi_y}$) from the guidance algorithm, the body angular rates from the rate gyros ($\dot{\phi}$), the measured vehicle attitude angles from the stabilized platform (ϕ), and the lateral accelerations ($\ddot{Y}$) from the body mounted accelerometers to solve for

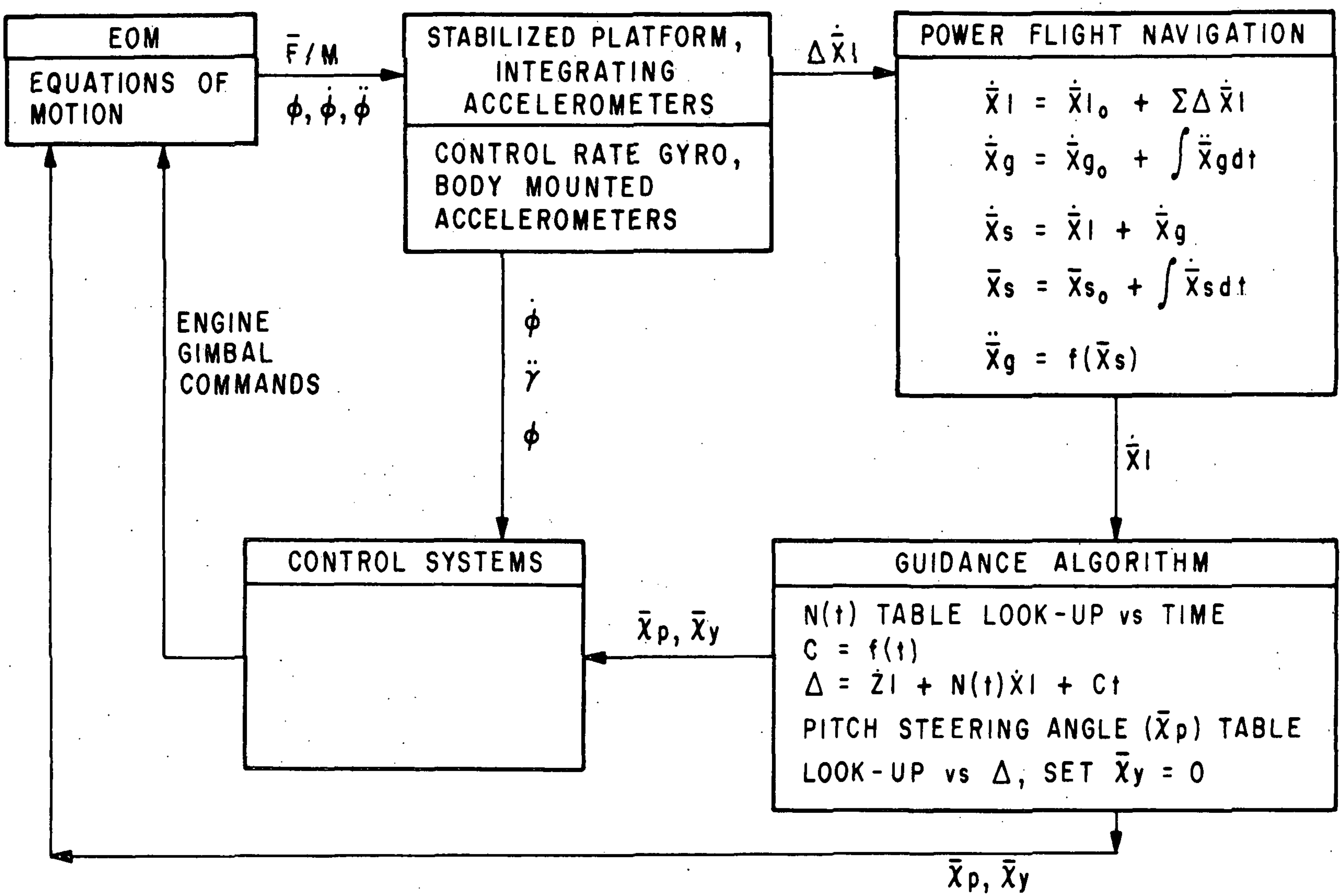

FIG. 9. FLOW DIAGRAM FOR GUIDANCE ANALYSIS

the engine gimbal angles. The equations of motion would use the sum of the moments in determining the body angular accelerations which must be integrated once to give body angular rates, and twice to give the attitude angles. Once the control equations and the recommended control gains have been identified, it is possible to solve for vehicle angles that satisfy both the control equations and steady-state moment balance. This type of steady-state moment-balance trajectory simulation will allow the engine gimbal angles and actual vehicle attitude angles to closely follow these same angular histories computed from a stable six-degree-of-freedom trajectory simulation. This level of steady-state trajectory simulation must be reached before a detailed guidance analysis has any meaning.

As stated earlier in the report, wind biasing of the trajectories used to establish the load relief guidance function will be addressed in this section. The flight geometry selected for this feasibility analysis is consistent with a 55 degree inclined orbit which uses a flight azimuth of 38 degrees. The wind data (wind magnitude and direction) used in conjunction with the ±4% thrust deviation boundary trajectories is illustrated by Figure 1. The ±4% F and nominal pitch steering profiles generated when these wind data are used in the trajectory shaping technique are shown by Figure 10. Observe that the angle-of-attack tilt-over (kick-over) program and resulting pitch steering profiles take on a slightly different shape from those of the non-wind biased trajectories illustrated by Figure 4. The inertial pitch plane velocity plots from the wind-biased ±4% F boundary trajectories that are used to derive the closed-loop velocity guidance algorithm is shown by Figure 11.

The velocity histories of Figure 11 were used to generate the variable Δ (defined in Section III) and plotted against the pitch steering angle as shown by the dashed curved line in Figure 12. The solid line represents the ±4% F non-wind biased boundary trajectory determined by the guidance function. Observe that the wind biased function lies very close to the non-wind biased function. This may help to explain why wind biasing of this function may not be necessary to achieve a load relief state (data to be discussed later). The time varying coefficient [N(t)] for the wind biased function will not be shown since it is so close to the one shown by Figure 8.

The criteria selected as an aerodynamic loads indicator is defined to be the dynamic pressure (Q) times the angle-of-attack deviation from the zero lift aerodynamic state ($\Delta\alpha = |\alpha - \alpha_{ZL}|$). When the load relief guidance algorithm has been wind biased for the wind data as shown by Figure 1, the maximum $Q\Delta\alpha$ plotted against a wind speed parametric variation of the scale factor is given by Figure 13. A wind speed scale factor of 0.5 means that the wind speed given as a function of altitude in Figure 1 has been multiplied by 0.5. The ±4% F and nominal

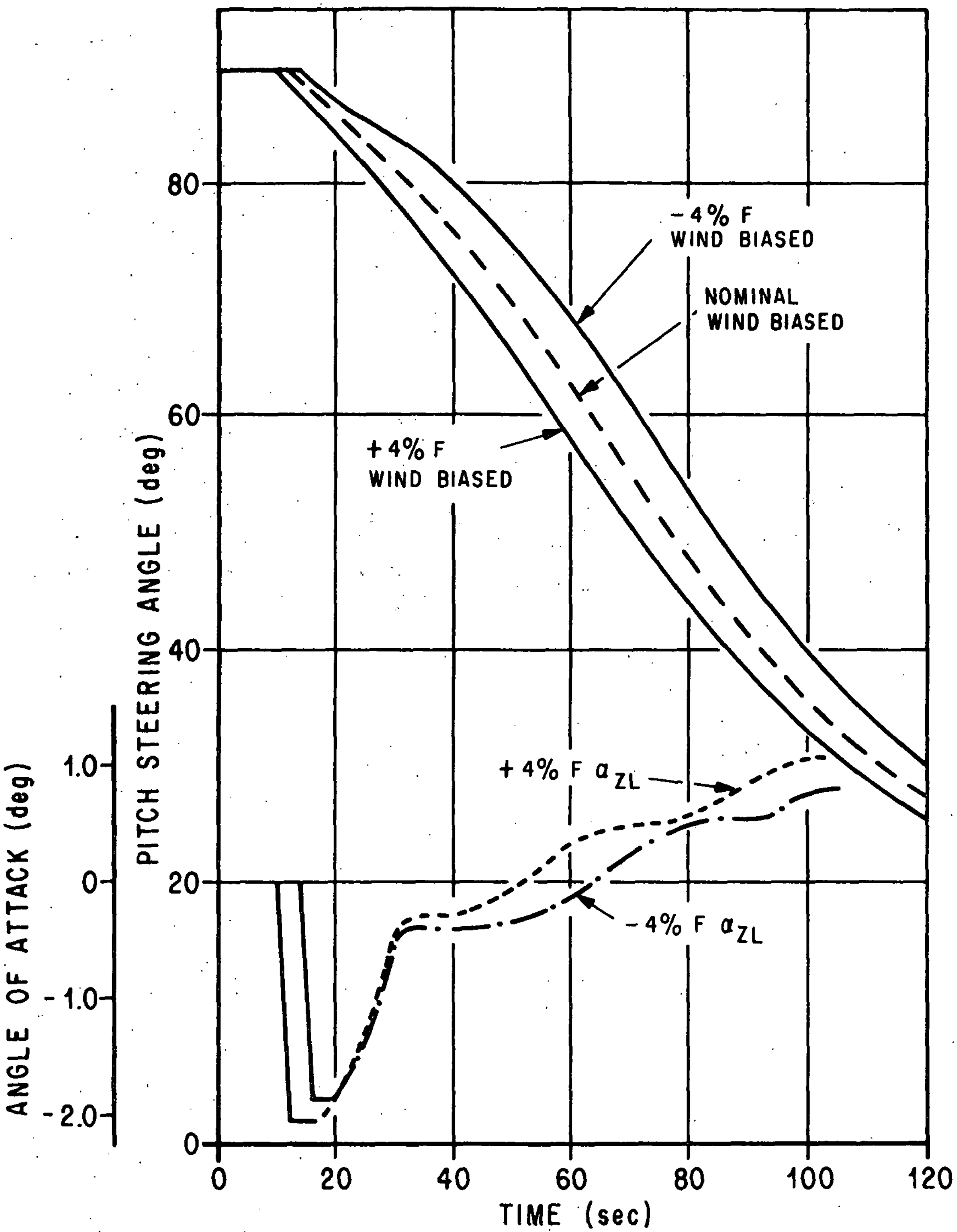

FIG. 10. ± 4% F AND WIND BIASED BOUNDARY CURVES

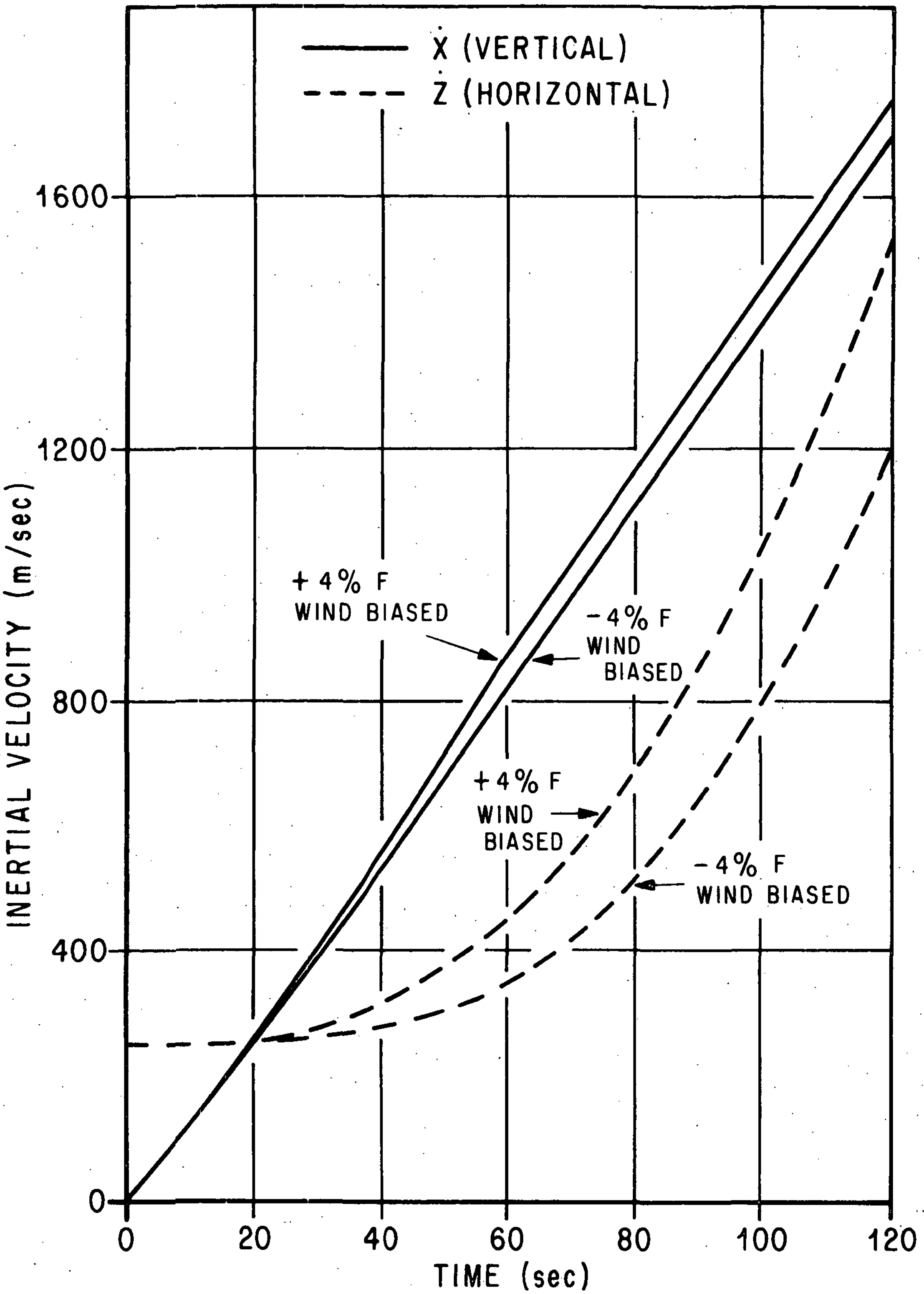

FIG. 11. ± 4% F WIND BIASED PITCH INERTIAL VELOCITY

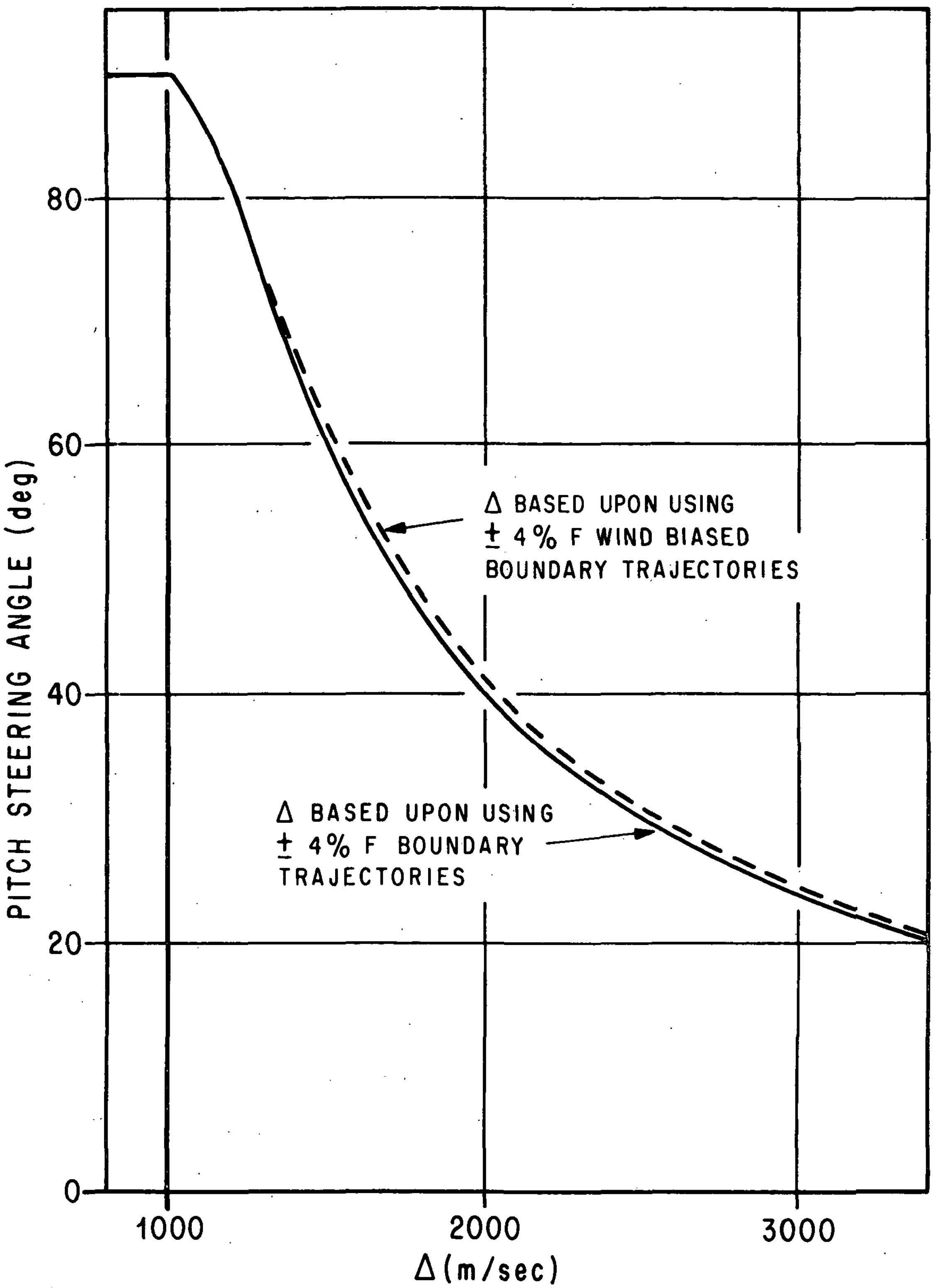

FIG. 12. PITCH STEERING ANGLE vs Δ

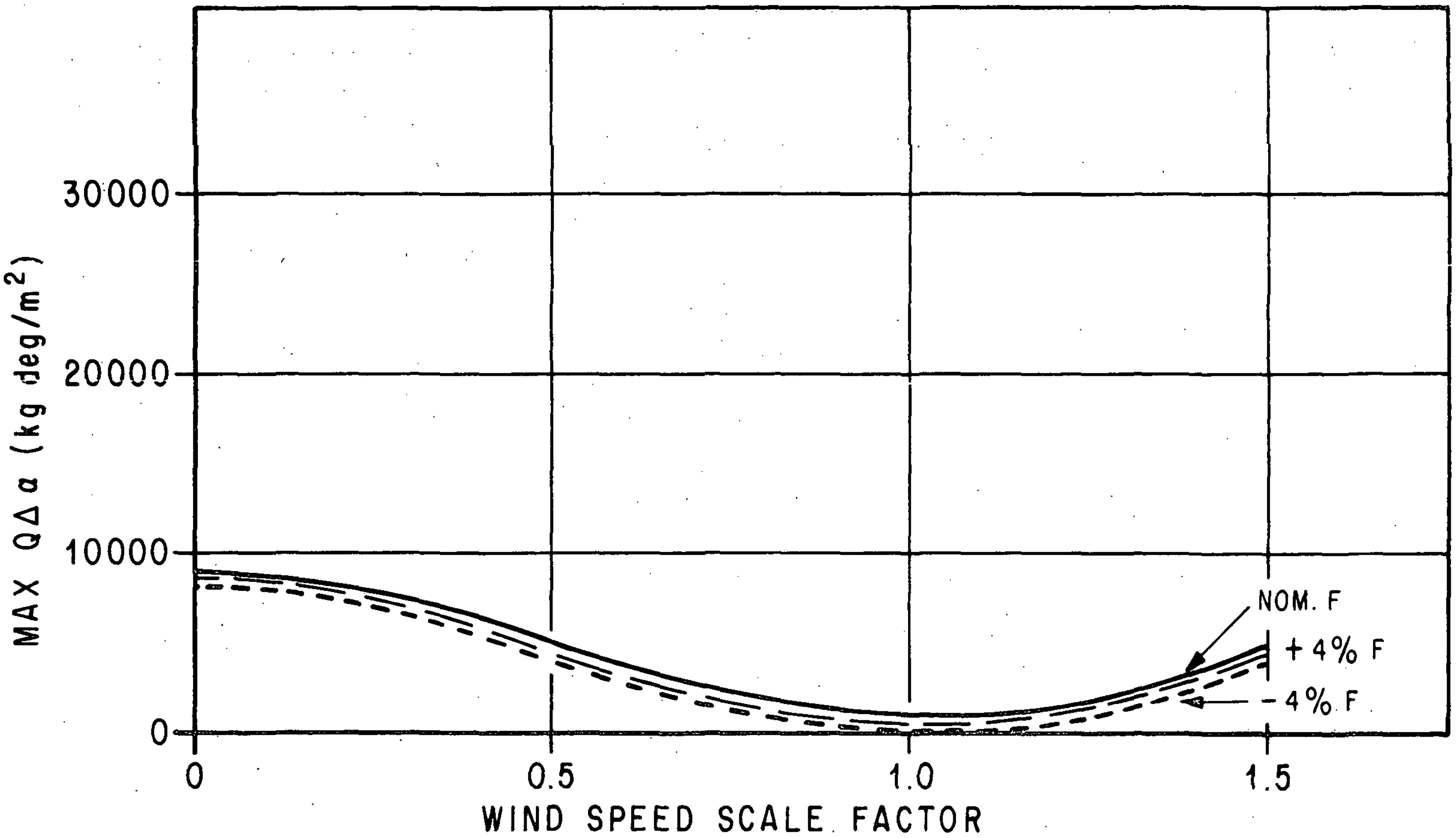

FIG. 13. SPACE SHUTTLE LOAD INDICATOR FOR CLOSED LOOP (WIND BIASED) ASCENT STEERING

thrust level trajectories were simulated for wind speed scale factors of 0 to 1.5* in increments of 0.25. Although the nominal did not appear in the derivation of the load relief guidance algorithm, the maximum $Q\Delta\alpha$ is only slightly higher than the ±4% F boundary trajectories. Observe that if the guidance algorithm was wind biased, and no wind occurred during that particular launch, the highest value of maximum $Q\Delta\alpha$ (8000 kg. deg/m^2) occurs for this condition. As would be expected, the loads for the design cases (±4% F and the wind speed scale factor equal to 1.0) are in the noise level of zero. The simulations were generated with the inertial velocity components (pitch plane) in a closed-loop mode of operation.

Figure 14 shows the same type of data for the open-loop (time dependent only) wind biased guidance function. The worst case (22500 kg.deg/m^2) from a loads standpoint occurs when the open-loop guidance function has been wind biased and no wind occurs on that launch day, and when the booster thrust is 4% low (-4% F). It should be noted that although the loads indicator for the design case (nominal thrust and wind speed scale factor equal to 1.0) are near zero, the -4% F case gives a maximum loads indicator value of about 13000 kg.deg/m^2 It should, again, be pointed out that these trajectories were simulated assuming perfect control and steady-state moment balance. The loads resulting from an active control system and full dynamics could be either greater or smaller depending upon the load relief properties of the control system.

Some insight into the agonizing question of whether or not to wind bias for an expected wind that was alluded to earlier in the report can be gained by examination of Figures 15 and 16. Figure 15 is a plot of the maximum $Q\Delta\alpha$ experienced by the space shuttle as the wind speed scale factor is varied from 0.0 to 1.5 when wind biasing is not used in the load relief guidance algorithm to determine the pitch steering angles during atmospheric ascent. Observe that the maximum load for a full value wind (scale factor = 1.0) is 10,000 kg.deg/m^2 and near zero for no winds. Now observe the consequences of failing to wind bias when using the open-loop guidance system to determine the pitch steering angles during atmospheric ascent (Figure 16). A full value wind (scale factor = 1) coupled with a +4% high thrust yields a maximum $Q\Delta\alpha$ of 40,000 kg.deg/m^2. This represents a factor of 4 greater loads for this particular set of conditions. This difficult decision of whether to wind bias or not usually occurs during the transition months of fall to winter (November to December) and winter to spring (March to April) when it is difficult to determine when the seasonal wind will change in magnitude and direction.

Since this load relief guidance algorithm has the built in property of responding to a perturbation according to the minimum load trajectory shaping technique, then it might not be necessary to compute a new

---

* A scale factor of 1.5 is approximately equivalent to a 95 percentile wind.

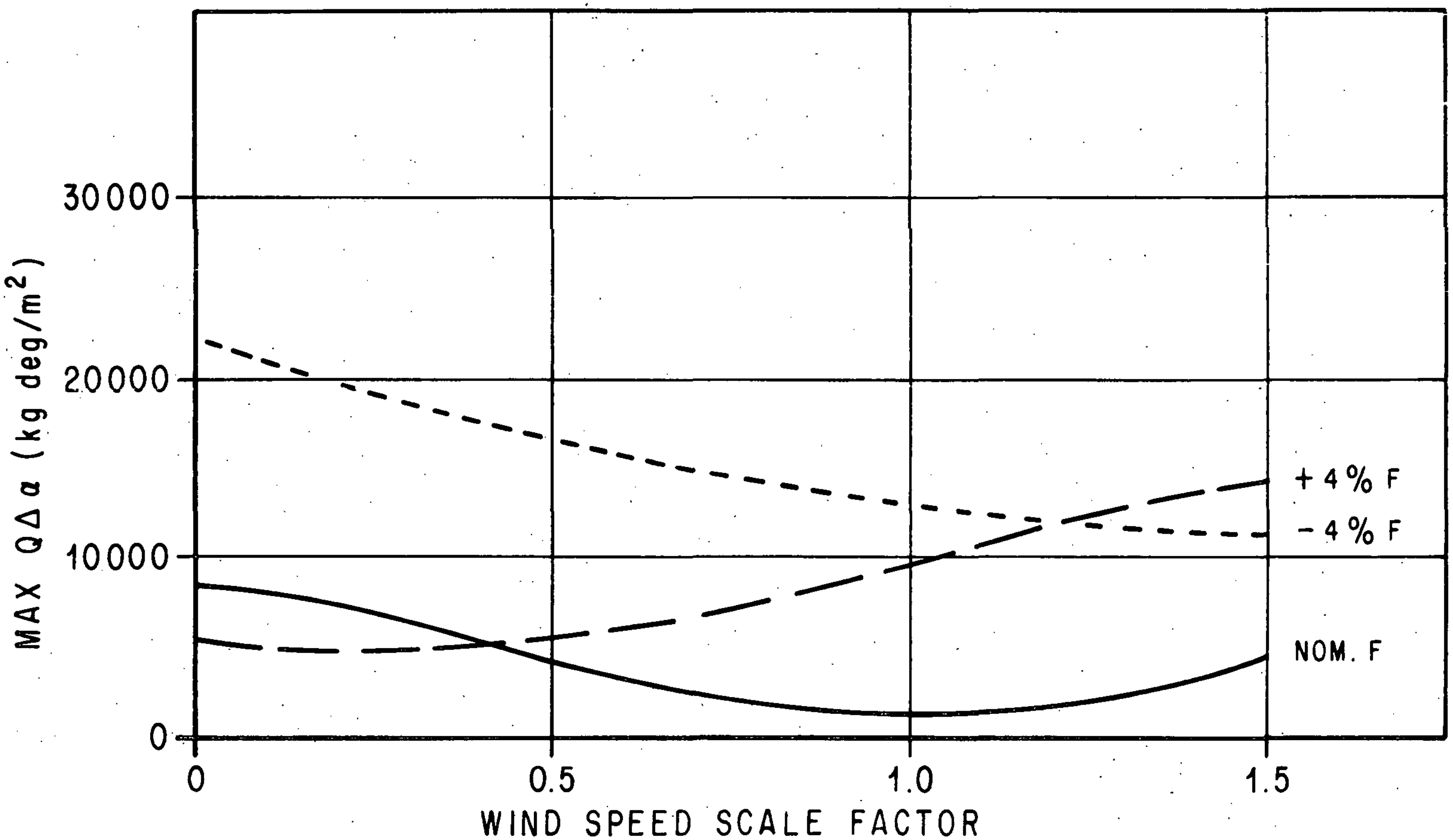

FIG. 14. SPACE SHUTTLE LOAD INDICATOR FOR OPEN LOOP (WIND BIASED) ASCENT STEERING

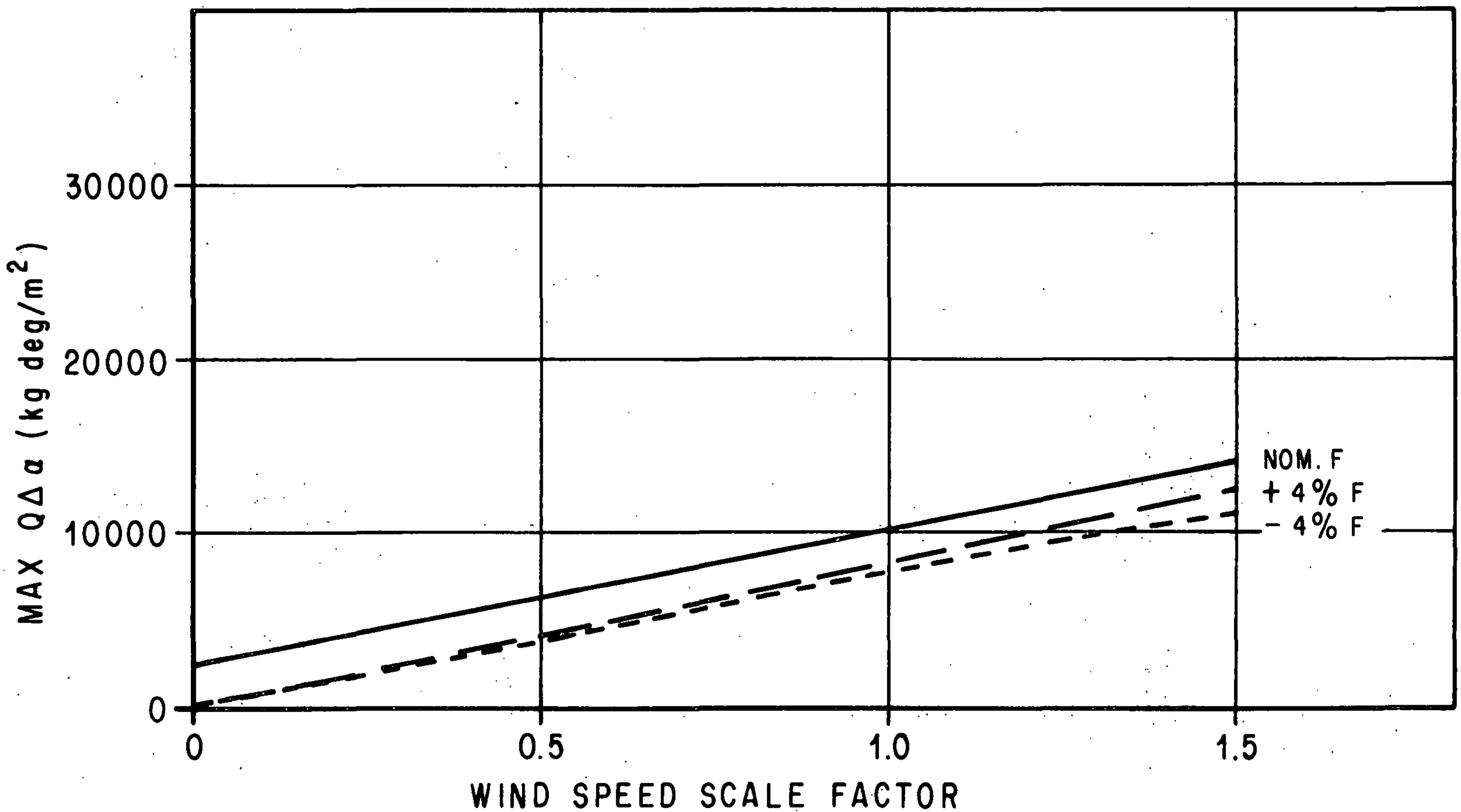

FIG. 15. SPACE SHUTTLE LOAD INDICATOR FOR CLOSED LOOP ASCENT STEERING, NO WIND BIAS

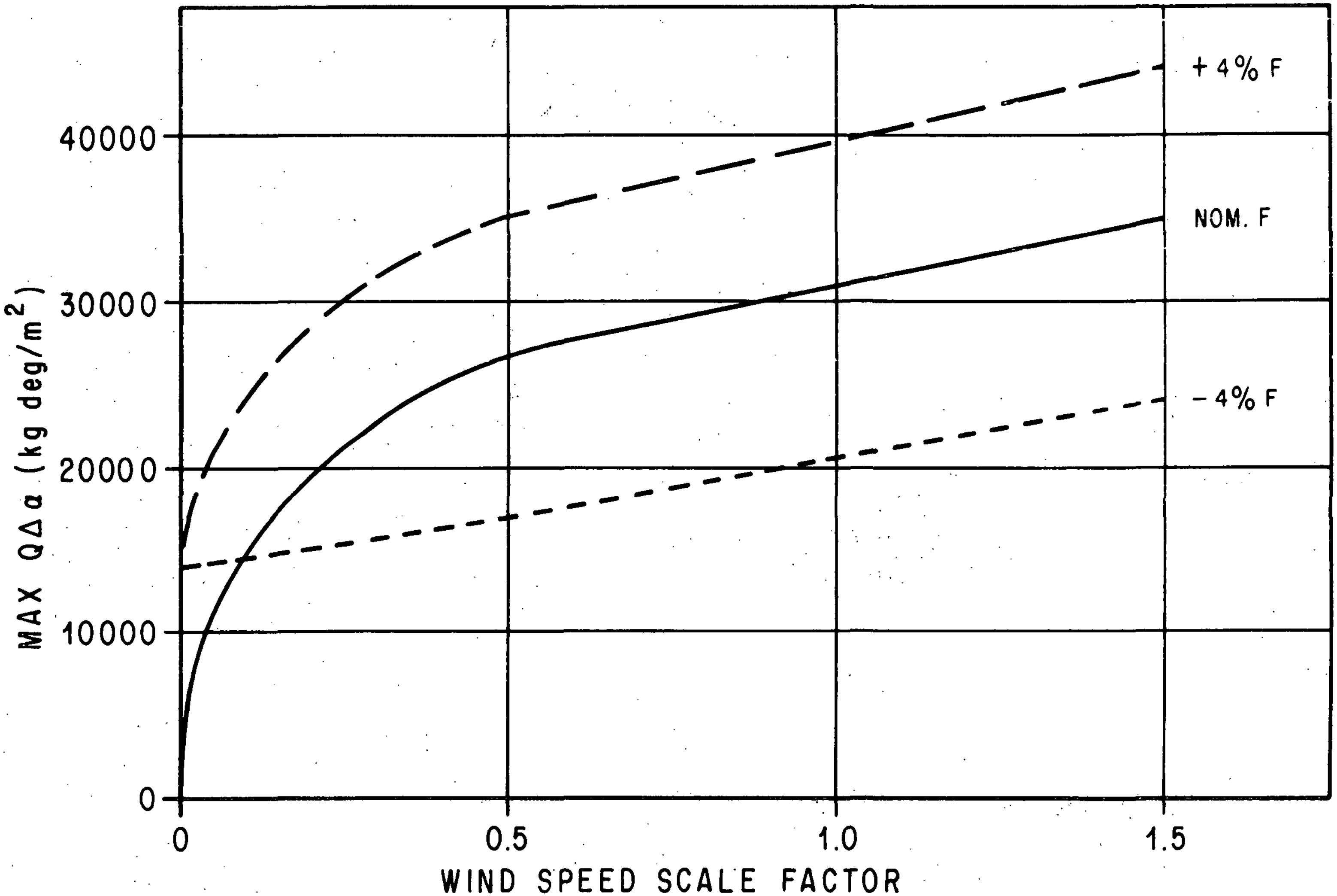

FIG. 16. SPACE SHUTTLE LOAD INDICATOR FOR OPEN LOOP ASCENT STEERING, NO WIND BIAS

guidance algorithm when the mission has been re-defined. An investigation indicated that a variation in liftoff weight of ±10,000 pounds has absolutely no influence on the maximum loads encountered during atmospheric flight, although the load relief guidance algorithm was not re-designed for the weight variation. A ±5% variation in the specific impulse (thrust held constant) of the propulsion system had negligible effect on the loads encountered. A launch azimuth change might cause the guidance algorithm to need redesigning when wind biasing is used, since the wind speed components in the pitch plane would differ as the launch azimuth varies.

V. CONCLUSIONS AND COMMENTS

The load relief guidance algorithm presented in this report meets all the requirements for an onboard ascent guidance scheme. The onboard computer requirements are near minimal and no additional navigational information is required. Wind biasing capability is available if needed. Steady-state moment-balance trajectory simulations of the proposed load relief guidance algorithm indicate that loads are reduced by a factor of 2 to 4 when compared to an open-loop (time dependent) guidance scheme for wind and thrust perturbations encountered during atmospheric ascent flight. The results are based upon an earlier MSFC pressure-fed booster and orbiter configuration; however, the basic trends should be applicable to the latest solid rocket motor booster/orbiter configuration. A study using the latest space shuttle configuration is underway.

The results presented in this report were for closed-loop steering only in the pitch plane. In future analysis, a yaw steering strategy will be considered in order to recover some of the performance lost due to out of plane velocity and displacement deviations.

An outline of the tasks to be pursued on the SRM booster/orbiter space shuttle configuration are given below:

1. Apply load relief guidance algorithm to latest SRM booster/orbiter space shuttle configuration.

2. Develop the guidance algorithm to include the displacement components.

3. Study yaw steering strategy.

4. Couple the guidance algorithm with a control system for detailed control analysis.

5. Redesign guidance algorithm to reflect the control system compatibility based upon task 4 study results (sensitivity analysis).

REFERENCES

1. Horn, Helmut J., "Application of an Iterative Guidance Mode to a Lunar Landing," NASA TN D-2967.

2. Geissler, E. D.; Chandler, D. C.; Deaton, A. W., "Adaptive Guidance for Saturn Vehicles," Congress Proceedings of XVII International Aeronautics Federation.

3. Smith, I. E., "General Formulation of the Iterative Guidance Mode," NASA TM X-53414.

4. Brown, S. C., "Cape Kennedy Wind Component Statistics Monthly and Annual Reference Periods for all Flight Azimuths from 0 to 70 km Altitude," NASA TM X-53956.

5. Smith, O. E., "Monthly Vector Mean Winds Versus Altitude for Cape Kennedy, Florida, for Skylab (INT-21) Wind Bias Trajectory Analysis," S&E-AERO-YT-77-71.

6. Deaton, A. W., "Adaptive Guidance for the Saturn Vehicle First Stage with Engine-Out Capability," MSFC, Aero-Astrodynamics Laboratory Internal Note No. 18-62.

APPROVAL

STRUCTURAL LOAD REDUCTION OF THE SPACE SHUTTLE
BOOSTER/ORBITER CONFIGURATION USING A LOAD RELIEF GUIDANCE TECHNIQUE

by A. W. Deaton and P. B. Kelley

The information in this report has been reviewed for security classification. Review of any information concerning Department of Defense or Atomic Energy Commission programs has been made by the MSFC Security Classification Officer. This report, in its entirety, has been determined to be unclassified.

This document has also been reviewed and approved for technical accuracy.

Clyde D. Baker

Clyde D. Baker, Chief
Astrodynamics & Guidance Theory Division

E. D. Geissler

E. D. Geissler, Director
Aero-Astrodynamics Laboratory

DISTRIBUTION

DIR
DEP-T
A&PS-PAT
A&PS-IP (2)
A&PS-IL (8)
A&PS-TU/Mr. Wiggins (6)

S&E-DIR/Dr. Weidner
S&E-DIR/Mr. Richard

S&E-AERO-DIR/Dr. Geissler
S&E-AERO-DIR/Mr. Horn

S&E-AERO-G/Mr. Baker
S&E-AERO-G/Dr. Blair
S&E-AERO-GG/Mr. Causey
S&E-AERO-GT/Mr. Redus
S&E-AERO-GA/Dr. Burns
S&E-AERO-GG/Mr. McLeish
S&E-AERO-GG/Mrs. Brandon
S&E-AERO-GG/Mr. Deaton (40)

S&E-AERO-M/Mr. Lindberg
S&E-AERO-M/Mr. Buckelew
S&E-AERO-M/Mr. Hardage
S&E-AERO-M/Mr. Phillips

S&E-AERO-D/Dr. Lovingood
S&E-AERO-D/Dr. Worley
S&E-AERO-D/Mr. Ryan
S&E-AERO-D/Mr. Mowery
S&E-AERO-D/Mr. Weisler
S&E-AERO-D/Mr. Hammer

S&E-ASTR-DIR/Mr. Moore
S&E-ASTR-S/Mr. Brooks
S&E-ASTR-S/Mr. Deaton
S&E-ASTR-S/Mr. Brown
S&E-ASTR-S/Mr. Ellsworth

S&E-ASTR-X/Mr. Gilino

S&E-S/P/Mr. Swalley

PD-DO/Mr. Young
PD-DO/Mr. Goldsby (2)
PD-DO/Mrs. Reisz
PD-DO/Mr. Wheeler

S&E-ASTN-A/Mr. Coldwater
S&E-ASTN-AA/Mr. Lifer
S&E-ASTN-ADL/Mr. Bullock
S&E-ASTN-A/Mr. Sterett
S&E-ASTN-X/Mr. Hoodless
S&E-ASTN-X/Mr. Verble
S&E-ASTN-E/Mr. Kroll
S&E-ASTN-X/Mr. McCool

SP-MGR/Mr. Godfrey
SP-EM-MGR/Dr. Thomason
SP-EM/Mr. Thionnet
SP-SRB/Mr. Burks
SP-ET/Mr. Odom

PD-DIR/Mr. Jean

Air Force Flight Dynamics Laboratory
Wright-Patterson AFB, Ohio 45433
Attn: Mr. Westbrook/FDCC
Mr. Blatt/FDCL

Johnson Space Center
Houston, TX
Attn: Mr. Ken Cox (4)
Mr. R. Nobles

Scientific & Technical Info. Facility (25)
P. O. Box 33
College Park, Maryland 20740
Attn: NASA Rep. (S-AK/RKT)

Rockwell International Corporation
12214 Lakewood Blvd.
Downey, CA 90241
Attn: Mr. Loyde Stockwell
Mr. Tom Logsdon
Mr. David A. Engles

NASA Headquarters
Washington, D. C. 20546
Attn: Mr. Meyers/M
Mr. Donlan/MD-T
Mr. D. Michel/RWS
Mr. Carley/MTE
Mr. E. Livingston/MTG
Mr. T. Michaels/REG